Science Advances
AAAS

Supplementary Materials for

Ciliary protein Kif7 regulates Gli and Ezh2 for initiating the neuronal differentiation of enteric neural crest cells during development

Frank Pui-Ling Lai, Zhixin Li, Tingwen Zhou, Adrian On Wah Leung, Sin-Ting Lau, Kathy Nga-Chu Lui, William Yu-Ming Wong, Pak-Chung Sham, Chi-Chung Hui, Elly Sau-Wai Ngan*

*Corresponding author. Email: engan@hku.hk

Published 13 October 2021, *Sci. Adv.* **7**, eabf7472 (2021)
DOI: 10.1126/sciadv.abf7472

The PDF file includes:

Figs. S1 to S7
Tables S4 to S6

Other Supplementary Material for this manuscript includes the following:

Tables S1 to S3
Movies S1 and S2

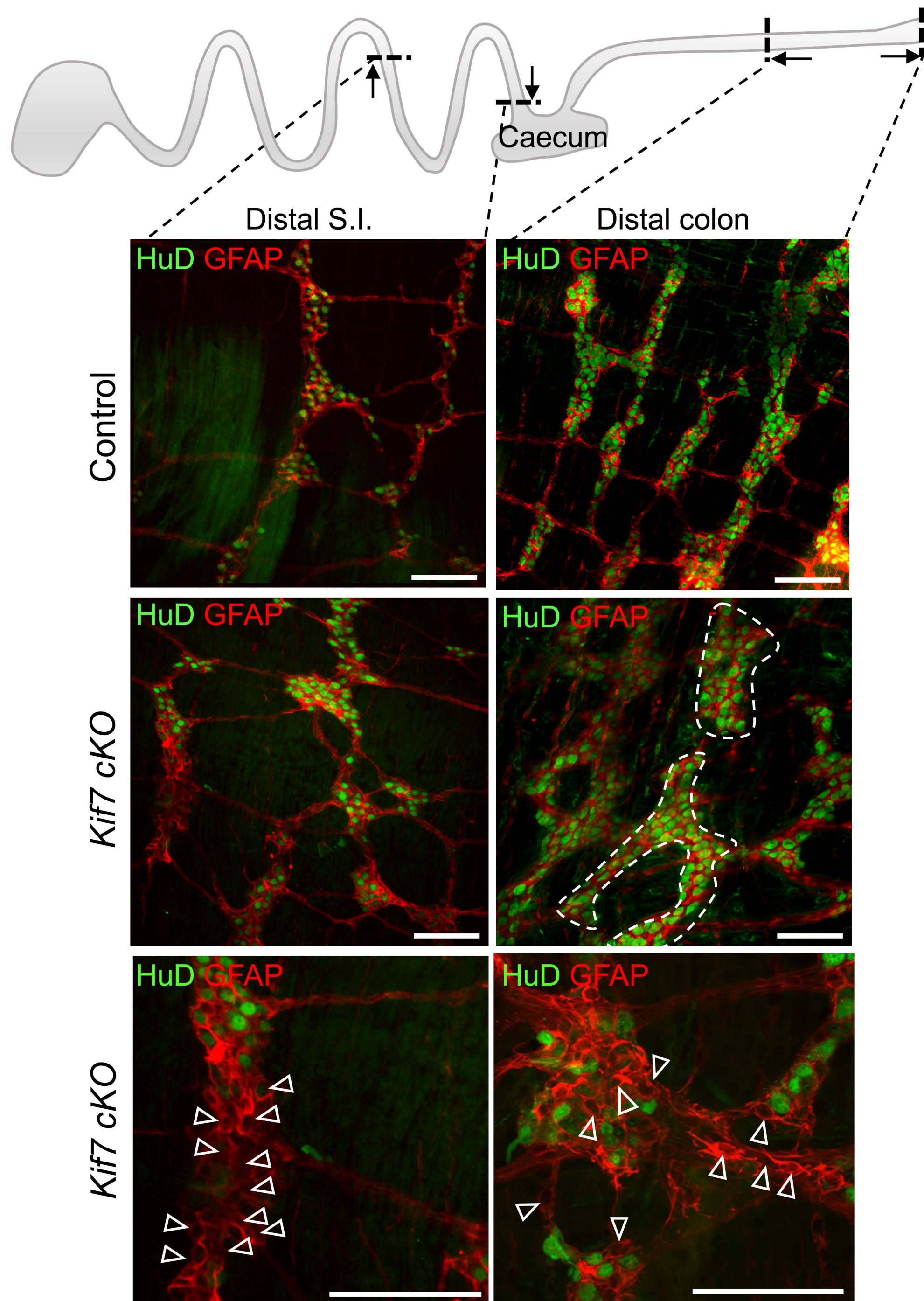

Fig. S1. Organization of myenteric plexuses in the distal small intestine (S.I.) and colon of the Control and *Kif7 cKO* (P21). The neurons and glia were marked by HuD and GFAP, respectively. Giant ganglion was found in *Kif7 cKO as* marked by dotted line. Neurons were outnumbered by glia in some enteric ganglia of the bowels of *Kif7 cKO* mice as marked by open arrow heads.

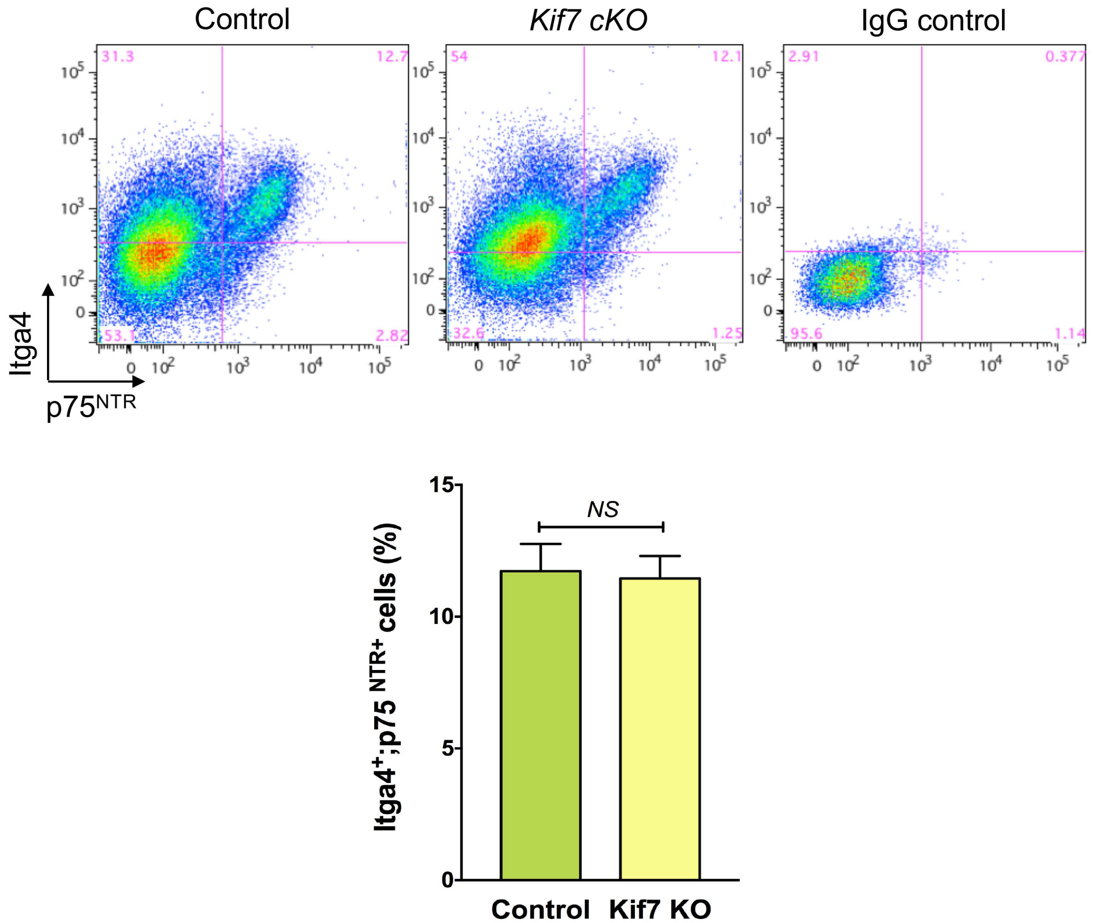

Fig. S2. Comparable numbers of ENCCs were found in E13.5 control and Kif7 cKO guts. ENCCs were detected using Itga4 and $p75^{NTR}$ antibodies and analyzed using flow cytometry. Bar chart shows percentages of $Itga4^{+}$;$p75^{NTR+}$ ENCCs over the total number of cells in E13.5 guts.

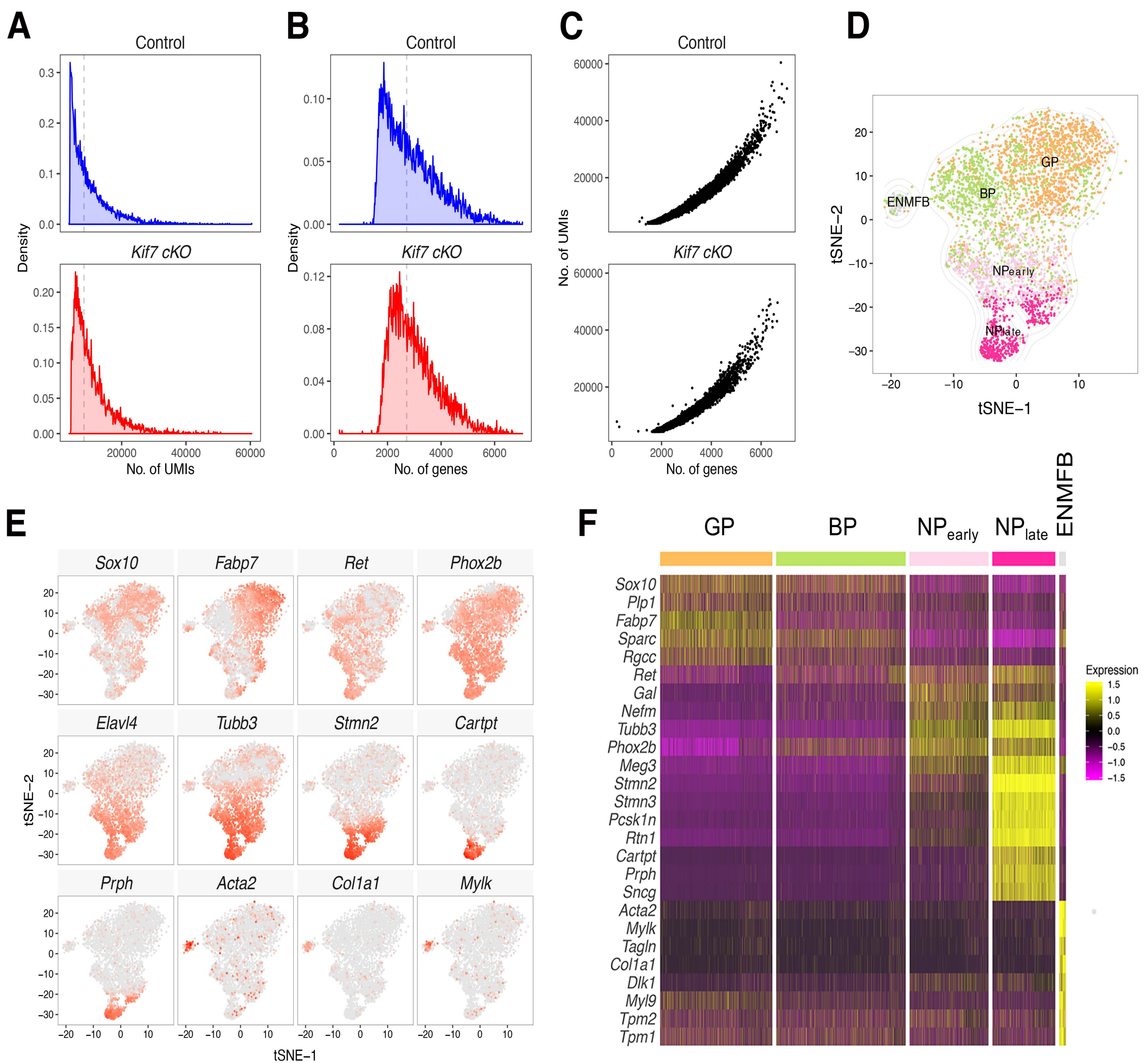

Fig. S3. High-resolution Dissection of ENCC Differentiation from Bipotent Progenitor Cells to Neuronal and Glial lineages by scRNA-Seq

(A) Distribution of the number of unique molecular identifiers (UMIs) detected per cell. Cells with more than 6,000 UMIs, but less than 60,000 UMIs, were selected for down stream analysis.

(B) Distribution of the number of genes detected per cell. Cells with more than 200 genes, but less than 10,000 genes, were selected for down stream analysis.

(C) Number of genes and UMIs detected per cell.

(D) Identification of 5 heterogeneous cell clusters (GP: Glial progenitor, BP: Bipotent progenitor, NP_{early}: Neuronal progenitor at early stage, NP_{late}: Neuronal progenitor at late stage, ENMFB: Enteric mesothelial fibroblast), colored by inferred cell types. Control and *Kif7 cKO* ENCCs were integrated together and shown in t-SNE plot.

(E) t-SNE projection of key markers in different clusters.

(F) Heatmap showing top markers identified by unsupervised method in different clusters.

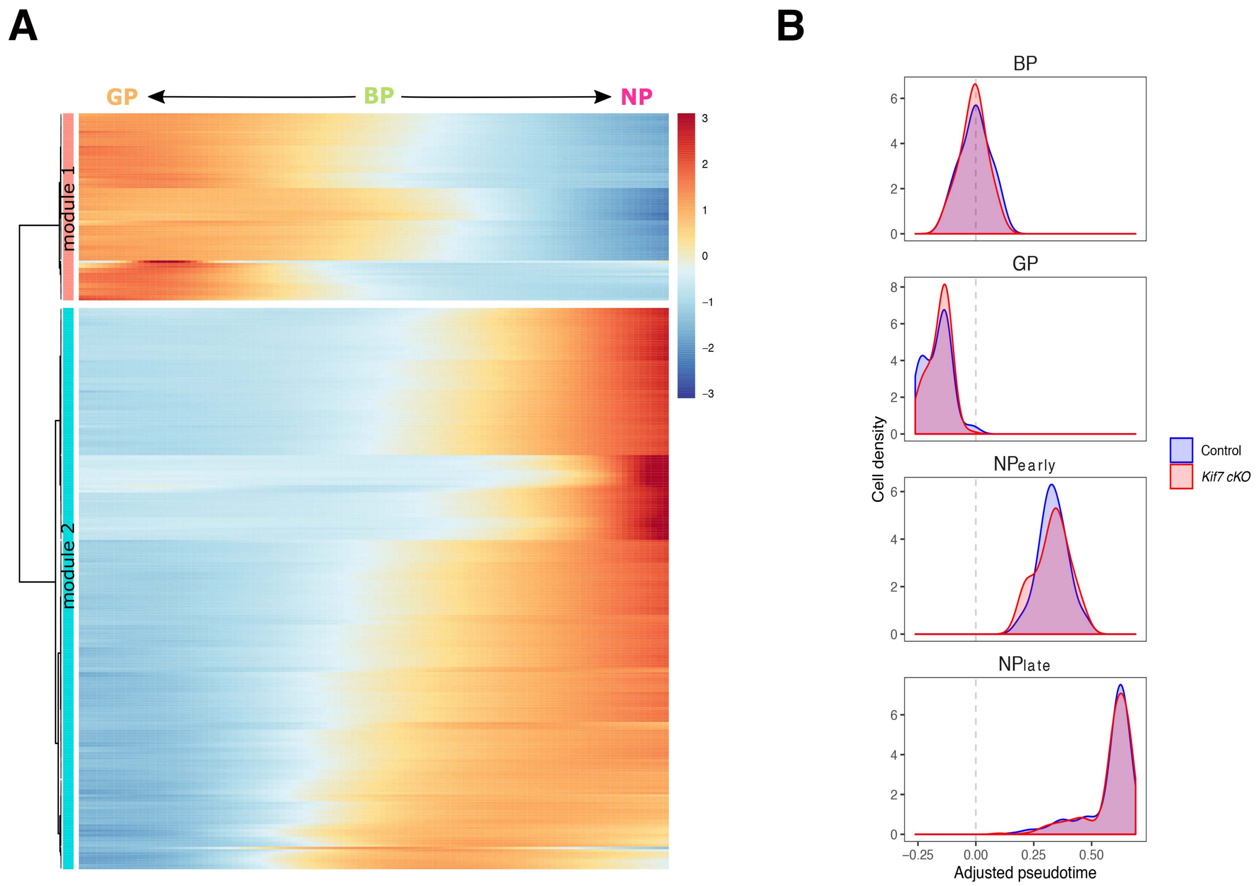

Fig. S4. Reconstruction of ENCC differentiation trajectory in a pseudotime manner
(A) Two clusters of dynamic genes during neuronal and glial lineage commitment.
(B) Density plot showing BP and GP population increased, while NP population decreased in *Kif7 cKO* mutant cells.

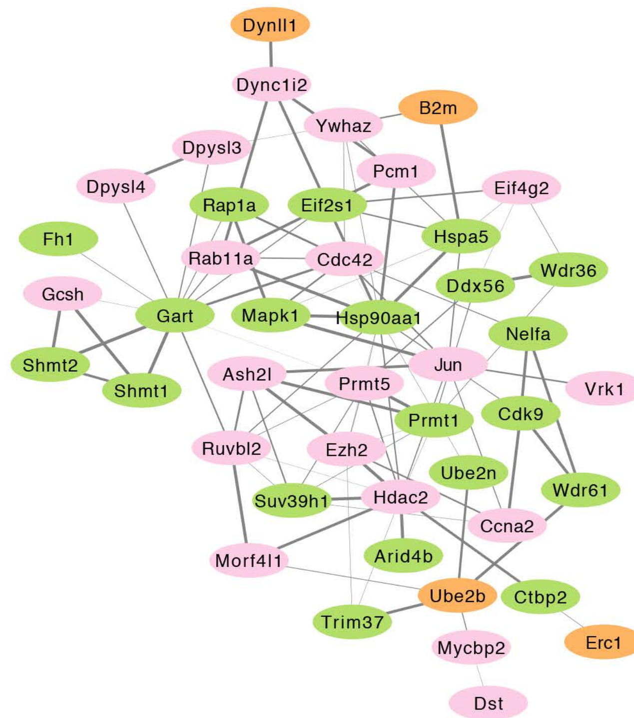

Figure S5. Protein-protein interaction network of the Ezh2 target genes in the core gene set. Protein interactions among the Ezh2 targets in the core gene set identified in *Kif7 cKO* ENCCs and their interactome, based on STRING database. Proteins implicated in BP, NP and GP are marked in green, pink and orange, respectively.

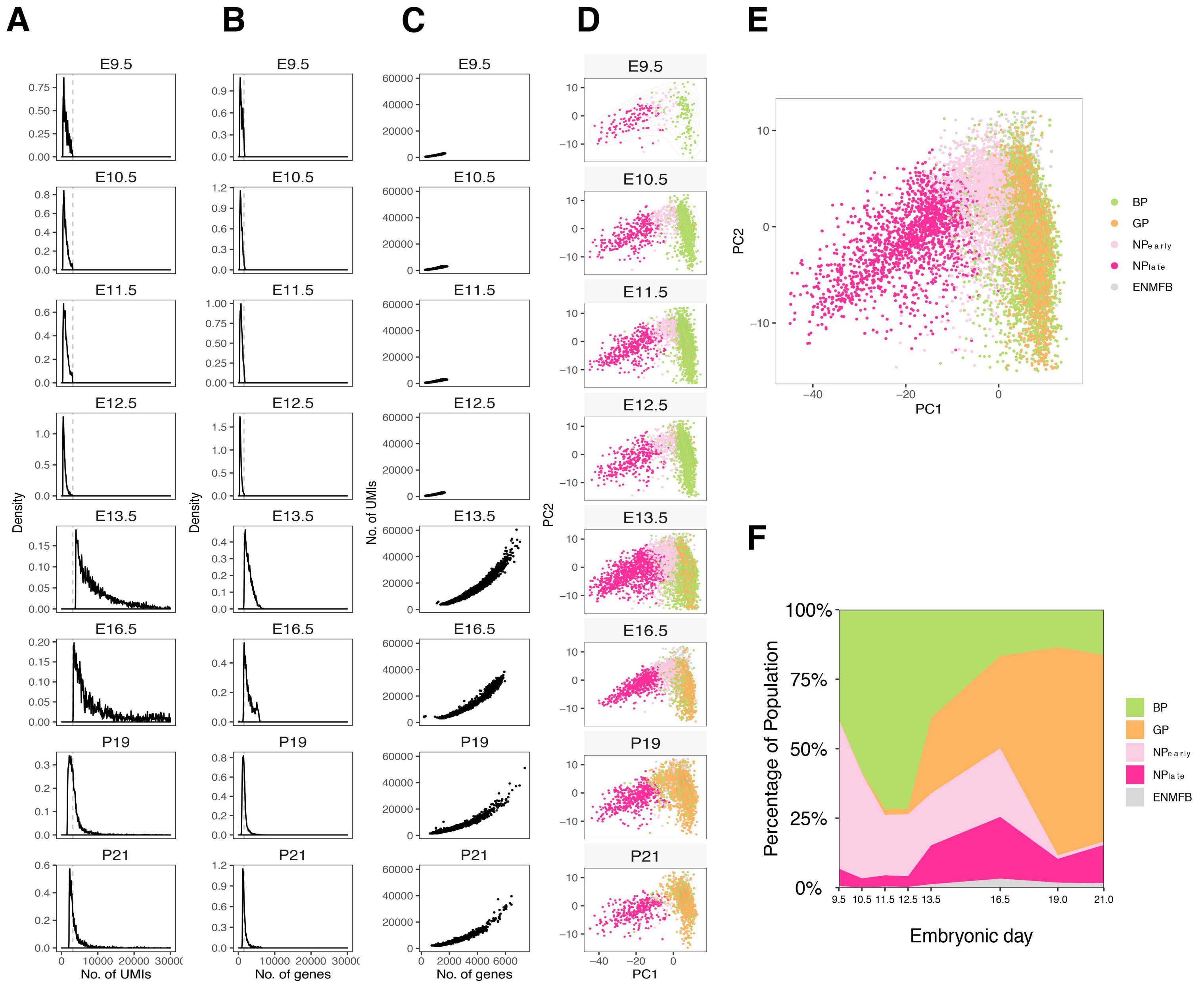

Fig. S6. Integration of ENCCs from different stages and multiple platforms

(A) Distribution of the number of unique molecular identifiers (UMIs) detected per cell across different stages. ENCCs at E9.5 to E12.5 were downloaded from MOCA database (24) which using the Sci-RNA-Seq3 platform. ENCCs at E13.5 to E16.5 were sequenced by our group using standard 10x Genomics platform. ENCCs at P19 to P21 were downloaded from Mouse brain atlas database (22) which using the 10x Genomics platform.

(B) Distribution of the number of genes detected per cell across different stages.

(C) Number of genes and UMIs detected per cell across different stages.

(D) Identification of 5 heterogeneous cell clusters (GP: Glial progenitor, BP: Bipotent progenitor, NP_{early}: Neuronal progenitor at early stage, NP_{late}: Neuronal progenitor at late stage, ENMFB: Enteric mesothelial fibroblast), colored by inferred cell types. ENCCs from 8 stages were integrated together and shown in PCA plot.

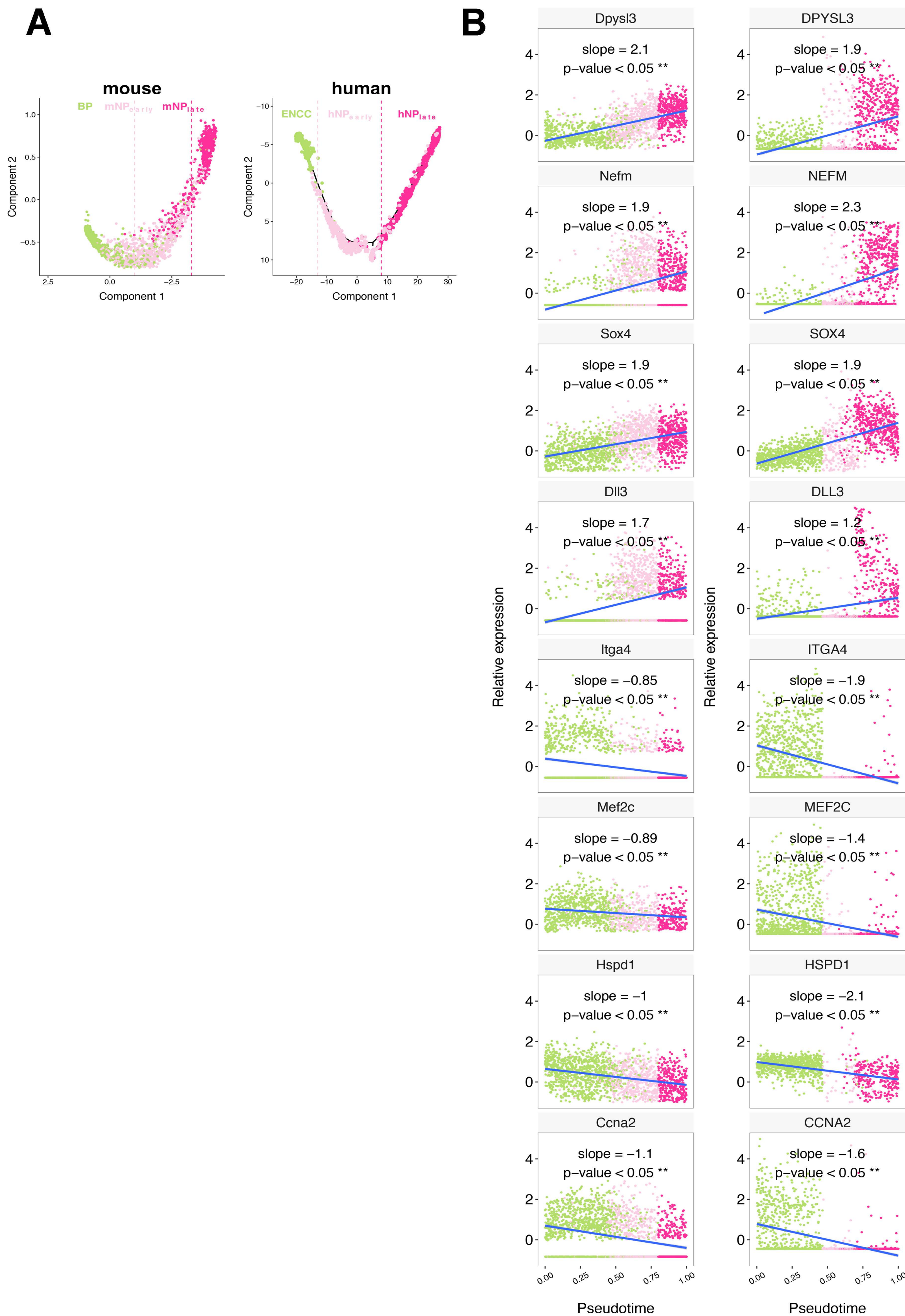

Fig. S7. Dynamic expression of the core genes along the neuronal lineage differentiation in mouse and human ENCCs. (A) Inferred neuronal differentiation trajectories of mouse and human ENCCs. **(B)** Dynamic expressions of the top 8 conservative genes in the core gene set along the neuronal lineage differentiation of mouse and human ENCCs. Linear regression (pseudotime as independent variables and gene expression as response variable) were fitted to show the change (slope) of gene expression along the pseudotime of development. Significances of regression (*P*-value) were shown in the scatter plots.

Mice
Wnt1-Cre, *ZE/G* and *Rosa26^{YFP}* mice were purchased from Jackson Lab. *Kif7$^{f/+}$* mice was kindly provided by C. Lobe, University of Toronto. *Gli2$^{f/+}$* was previously generated(*45*). Mice were maintained in a mix outbred background of C57 and 129/S6. Animals were kept in the Animal Laboratory of the University of Hong Kong, and all experiments were performed in accordance with procedures approved by the committee on the Use of Live Animals, the University of Hong Kong (CULTRA 3792-15).

Spatiotemporal mapping of colonic motility
Colons of 3- to 4-week old *Kif7 KO* and control littermates were dissected out and pinned to the chamber filled with oxygenated (95% O_2 and 5% CO_2) physiological saline solution flow. The composition of physiological saline solution is: NaCl 6.9 g/L, KCl 0.34 g/L, NaH_2PO_4, 0.156 g/L, $MgSO_4$ 0.256 g/L, $CaCl_2$ 0.278 g/L, D-glucose 1.98 g/L, $NaHCO_3$ 2.1 g/L. Whole chamber was incubated in 37°C water bath as previously described(*46*). After 30 minutes of equilibration, mouse stool was inserted into the oral end of colon and movies of gut motility were captured at 30 frames per second using a digital camera (Stylus Tough, Olympus Inc.). Individual frames from the captured videos were then converted into spatiotemporal plots using ImageJ Software. The bowel's edges were then computed and used to determine the gut motility. The resulting spatiotemporal map allows us to characterize the colonic migrating motor complexes (CMMCs), which constitute the recurrent ENS-mediated contractions propagating along the colon preparations. Stool movement speed was calculated as the time taken to expel fecal pellet from the oral to anal ends of the colon preparation over the length of the colon preparations. At least 6 samples in each group were examined and the mean values of the stool movement speed ± SEM were shown in the bar chart

Ex vivo gut contractility assay
Distal colon gut explants were harvested from 6-8 week-old control and mutant mice and placed in ice-cold HBSS. 10mm gut explants were suspended isometric-force organ-bath chambers filled with Krebs solution (117 mM NaCl; 4.7 mM KCl; 1.2 mM MgCl2; 1.2 mM NaH2PO4; 25 mM NaHCO3; 2.5 mM CaCl2, and 11 mM glucose), warmed at 37 °C and with 95% O2 + 5% CO2. After an equilibration period of 60 min, the gut explants were subjected to low-voltage electrical field stimulation (5-ms pulse at 30 V). The contractile response of the gut muscle was continuously recorded using a four-chamber tissue-organ bath with isometric-force transducers (AD Instruments) coupled to a computer equipped with LabChart Pro software (AD Instruments). The amplitudes of contraction were measured 120s after equilibration and the maximum contraction forces were calculated using the Peak Analysis package from LabChart Pro software.

Adult myenteric plexus preparation and immunostaining
The gastrointestinal tract was dissected out from the 3- to 4-week old mice, washed by cold phosphate-buffered saline, opened by cutting along longitudinal tract border, pinned serosa side down on dish covered with agar gel. After fixation in 4% paraformaldehyde in phosphate-buffered saline 2 hours at 4°C, mucosa layer was removed from muscle layers containing myenteric plexus using extremely fine point forceps under dissection microscope. Samples from distal small intestine and colon were cut into 1 cm segments and stored in 1x phosphate-buffered saline at 4°C.
Myenteric plexus segments were permeabilized in TBST containing (100 mM Tris, 150 mM NaCl, 1% Triton X-100) 1 hour at room temperature and blocked with TBST containing 10% FBS, 0.2% Sodium Azide 18 hours at 4°C. Subsequently, these segments were incubated with primary and secondary antibodies as listed in Table S1 & 2.

Immunofluorescence

Embryos and guts were fixed in 4% paraformaldehyde in phosphate-buffered saline for 4 hours at 4°C, dehydrated in 30% sucrose in phosphate-buffered saline overnight at 4°C, embedded in OCT (Tissue-Tek). For immunohistochemistry, the sections were blocked in phosphate-buffered saline containing 10% normal goat serum or fetal bovine serum and 0.1% Triton X-100 for 2 hours at room temperature and then incubated in primary antibody overnight at 4°C. The primary antibodies listed in Tables S1 & 2. For immunocytochemistry, the cells were fixed with 4% paraformaldehyde in PBS at room temperature for 30 min, followed by blocking with 1% bovine serum albumin (BSA) (Thermo Scientific, 23209) with or without 0.1% Triton X-100 (Sigma, T8787) in PBS buffer. Cells were then incubated in primary antibody overnight at 4°C and host-appropriate Alexa Fluor -488 or 594 secondary antibody (Molecular Probes, Invitrogen) (Table S2) for 1 h at room temperature. Cells were then counterstained with mounting medium with DAPI (Thermo Scientific, P36931) to detect nuclei. Cells were photographed using Carl Zeiss confocal microscope (LSM 800). Quantitative image analysis of differentiated neuronal cultures was performed with ImageJ. A minimum of 300 cells were analyzed per sample. Percentages of neuronal cells were measured over the total number of cells (DAPI) and the values reported in bar charts represent the mean ± SEM. These sections photographs were captured using Carl Zeiss LSM 800 confocal laser scanning microscope.

Gut Explant Cultures and Time-Lapse Imaging

For gut migration studies, guts were dissected out from E12.5 mouse embryos of YFP genetic background. Whole guts were placed on a filter paper (Millipore, Billerica, MA) and cultured with DMEM medium containing 10% fetal bovine serum, 0.075% sodium bicarbonate, and L-glutamine in a heat- and humidity-controlled chamber of 5% CO_2, 37°C. Images were captured using a Carl Zeiss LSM 800 laser scanning confocal microscope. Images were collected as Z stacks with a Z step size at 4μm and all images were rendered for maximum intensity projection with ZEN software (Carl Zeiss). Individual enteric NCCs in gut explants were tracked using ImageJ software to determine their speed of locomotion and persistence of movement. The speed of each cell was determined by dividing the total length of its trajectory by the time (a minimum of 14 hours was measured). The net speed of each cell was determined by dividing the distance between its initial and final position by the time. Persistence was obtained by dividing the distance between its initial and final position by the total distance covered by the cell.

Flow cytometry analysis

For flow cytometry analysis, E13.5 embryonic guts were dissociated with dispase Ⅰ and collagenase (1 mg/mL, 0.4 mg/mL) at 37°C for 5 minutes. The dissociated cells were then incubated with antibodies against Integrin4α and $p75^{NTR}$ for 30min at 4 °C. Approximately 10^6 labeled cells were acquired and analyzed using a FACSCalibur (Becton Dickinson Immunocytometry Systems, San Jose, CA, USA). Isotype-matched antibodies were used as controls. FlowJo version 8.2 (Tree Star, Inc.) was used to analyze flow data. A list of primary antibodies and working dilutions is provided in Tables S4 & S5.

Enteric neural crest cell culture

Enteric NCCs were isolated from E11.5 $Kif7^{f/f}$ embryonic guts. Guts were dissected in L15 medium and washed with phosphate-buffered saline. Guts were digested by Dispase Ⅰ and collagenase (1 mg/mL, 0.4 mg/mL) at 37°C for 5 minutes. Digested guts were triturated into single cells and spinned down. Cells were resuspended in neural crest cell medium, containing 15% chick embryo extract (Gembio), fibroblast growth factor (20 ng/mL; Sigma Aldrich),

epidermal growth factor (20 ng/mL; Sigma Aldrich), retinoic acid (35 ng/mL; Sigma Aldrich), N2 (1%), B27 (2%, Life technolognies), β-mercaptoethanol (50 mM; Sigma Aldrich), and plated onto wells coated with poly-D-lysine and fibronectin (50 μg/mL and 20 μg/mL) and enriched by multiple replating. The enteric NCCs at passage 3 were harvested for Western blot, RT-qPCR, bulk RNAseq analysis or seeded at 1 $\times 10^6$ cells per 15mm well (24-well plate) for the subsequent functional analyses.

Viral Transduction

Ad-GFP and Ad-Cre-GFP recombinase adenovirus (Vector Biolabs) was added to the second passage of ENCCs (in a dilution 1:100 and 1:30 respectively). Four days after infection, approximate 90-95% cells expressed GFP. Deletion of *Kif7* and activation of Hedgehog pathway was confirmed by reverse transcription PCR and Western blot.

In vitro differentiation assay for mouse ENCCs

To determine the differentiation capacity of ENCCs after deletion of *Kif7* in presence or absence of *miR124*, 1 $\times 10^6$ Ad-GFP or Ad-Cre-GFP recombinant adenovirus infected *Kif7$^{f/f}$* ENCCs were seeded per 15mm well with 1mL ENCC medium. The differentiation was induced by addition of GDNF (100ng/mL). One day after addition of GDNF, ENCCs were transfected with 20nM MISSION® *miR-124* mimic (HMI0085, CGUGUUCACAGCGGACCUUGAU, Sigma Aldrich) or *miRNA* negative control (HMC0003, CGGUACGAUCGCGGCGGGAUAUC) using 2μL LTX lipofectamine and 1μL PLUS reagent (Invitrogen) according to the standard protocol provided by the manufacturer. The ENCCs were cultured in the differentiation medium for 5 or 10 additional days in presence of GDNF or in combination of Ezh2 inhibitors: GSK126, 2.5μM (Abcam Cat. no.: ab269816) or EPZ-6438, 5μM (Abmole, Cat. no.: M2677-10) and then harvested for immunocytochemistry analyses with antibodies against the neuronal and glial markers as listed in Table S4 & S5. At least 3 independent experiments were performed. Sox10$^+$/Phox2b$^+$, Phox2b$^+$Sox10$^-$, Sox10$^+$/Phox2b$^-$ and Tuj1$^+$ cells were considered as BP, NP, GP and committed neurons, respectively.

Derivation of enteric neurons from human pluripotent stem cells (hPSC)

Human ENCCs were derived from hPSCs using protocols described previously(*36, 43, 44*). In brief, hPSCs were dissociated into single cell suspension by Accutase (Millipore) and plated on Matrigel-coated plate in a density of 4×10^4 cells cm^{-2} in ES cell medium containing 10 ng/mL fibroblast growth factor 2 (FGF2, Peprotech). The differentiation was started by replacing ES cell medium with KSR medium and gradually switched to N2 medium from day 4 to day 10. To differentiate hPSCs to hENCCs, the cells were treated with 100 nM LDN193189 (Stemgent) from day 0 to day 3, 10 μM SB431542 (Abcam) from day 0 to day 4, 3 μM CHIR99021 (Stemgent) from day 2 to day 10 and 1 μM retinoic acid from day 6 to day 10. At day 10, the cells were dissociated into single cell suspension by Accutase (Millipore) and subjected to fluorescence-activated cell sorting (FACS). hENCCs which were positive to both HNK-1 (BD Biosciences) and p75^{NTR} (Miltenyi Biotec) were sorted by BD FACSAria III Cell Sorter. 5×10^4 sorted cells were seeded as droplets on polyornithine/laminin/fibronectin-coated surface. Neuronal differentiation was initiated by replacing the medium with N2 medium containing 10 ng/mL BDNF (Peprotech), 10 ng/mL GDNF (Peprotech), 10 ng/mL NT-3 (Peprotech), 10 ng/mL NGF (Peprotech), 1 μM dibutyryl cAMP (Sigma-Aldrich) and 200 μM ascorbic acid (Sigma-Aldrich). To examine the effect of Ezh2 inhibitor on neuronal

differentiation of hENCCs, hENCCs were cultured in differentiated medium in absence or presence of Ezh2 inhibitors: GSK126, 2.5μM or EPZ-6438, 5μM for 5 days. The differentiation was monitored based on the expressions of TUJ1/HU as revealed by immunocytochemistry.

Immunoblot
To detect the activation of Hedgehog signaling in enteric NCCs transfected by adenovirus, cells in 10 wells of 24 well dish were collected and lysed with lysis buffer (cell signaling technology). Cell lysates containing 50μg total protein were separated on 8% sodium dodecylsulfate polyacrylamide gels and transferred onto polyvinylidene fluoride membranes. The membranes were incubated with antibodies against Gli1 (1:500, Santa Cruze Biotechnology), Gli2 (1:500, R&D) and Gli3 (1:500, Santa Cruze Biotechnology). Anti- β-Actin (1:20000, Millipore) was used as loading control. All blots were incubated with1:2000 of polyclonal HRP conjugated anti-mouse, anti-rabbit or anti-goat secondary antibody (Dako Cytomation). Antibody-bound proteins were visualized using a Western Bright ECL HRP substrate (Adavansta).

Reverse Transcription
Total RNA was extracted from control and *Kif7*$^{-/-}$ enteric NCCs using RNeasy Mini Kit (Qiagen) and reverse transcribed in 10μL reaction system using Prime Script RT Master mix (Takara) in accordance with manufacturer's instruction. cDNAs were then used to perform quantitative PCR.

Quantitative Reverse Transcription Polymerase Chain Reaction (qRT-PCR)
Quantitative PCR was performed in the TaqMan (Thermo Fisher Scientific) or the SYBR Green reaction mix (Applied Bio-systems), which consisted of 1x Master mix, forward and reverse quantitative PCR primers as listed in Table S6. The reaction mix (19μL) was aliquoted into tubes and 1 μL complementary DNA was added. Triplicated 20μL samples and negative (water) controls were placed in a 96 wells PCR plate. The quantitative PCRs were performed using a ViiA 7 Real-Time PCR System (Thermo Fisher Scientific). Data were analyzed and processed using Sequence Detector version 1.6.3 (Applied Biosystems) in accordance with the manufacturer's instructions. Results were analyzed using the $2^{-\Delta\Delta CT}$ method and expressed relative to the control. 18S was used as the internal control. The values reported in bar charts represent the mean ± SEM and the experiments were repeated in three independent assays.

Extraction of mirRNA and qRT-PCR
Total RNA was extracted using the mirVana miRNA extraction kit (Thermo Fisher Scientific, Waltham, MA, USA) according to manufacturer's protocol. In brief, ~$2x10^5$ cells were lysed in 300μL of binding solution and 1/10 volume of homogenate additive followed by equal volume of acid-phenol:chloroform extraction. Add 1.25 volume of 100% ethanol and pass the mixture through the filter cartridge and wash once 700uL of wash solution 1, followed by two times washes with sol 2/3. Total RNA was eluted with 100uL of 100μL elution solution (Pre-heated to 95°C) with a RT was performed using the Taqman mirRNA reverse transcription kit (Thermo Fisher Scientific, Waltham, MA, USA) according to manufacturer's protocol. In brief, 7μL of RT reaction mix and 3μL of RT primer (miR-124a; #001182 and snoRNA202; #001232 were purchased from Thermo Fisher Scientific, Waltham, MA, USA) were added to 5μL RNA (~10ng) followed by thermocycler reaction as follows: 16°C for 30 mins; 37°C for 30 mins; 85°C for 5 mins. TaqMan q-PCR was performed using TaqMan Small RNA Assays for miR-124a and snoRNA202 (loading control) (Thermo Fisher Scientific, Waltham, MA, USA).

Reactions were performed in triplicate with cycling conditions as follows: 95°C for 30 seconds then 95°C for 15 seconds, 55°C for 10 seconds, and 72°C for 30 seconds, repeated 42 times. The Ct values were < 35 and Δct was calculated and normalized using loading control snoRNA202.

Bulk RNA sequencing

RNA sequencing was performed using RNA obtained from the control and *Kif7*$^{-/-}$ ENCCs in the Centre of Genomic Science, the University of Hong Kong. For the RNA-seq analysis, more than 35 million reads of each RNA-seq sample were aligned to mouse genome assembly GRCm38 (gencode Release M15 - GRCm38.p5). Raw sequence quality was assessed using FastQC(*47*). STAR(*48*) and RSEM(*49*) were used respectively to perform the paired-end alignment and estimation of expression levels (transcript per million, TPM). Only unique alignments to the genome were allowed.

The differential expression (DE) analyses were performed using EBSeq(*50*). Reads for each sample were normalized by the EBSeq method of median normalization. In the first time, samples were used as non-replicates because of significant differences in their gene expression level. From each pair of the control and *Kif7KO* ENCC, we generated a list of DEGs and then compared them to obtain the common DEG list among the 4 groups. A fold change cut-off of >=1.5 was used for each DEGs. *P*-value was calculated between the means of each replicate groups using t-test method. The significance level was set at 0.05 for false discovery rate (FDR)-corrected p-values. Gene enrichment analysis for DEGs was performed using DAVID(*51*), Gene Set Analysis Toolkit (GSAT)(*52*) and Gene Set Enrichment Analysis (GSEA)(*53*).

MA plot displaying expression and DE data was generated using *ggpubr* package from R. The mean log2 fold change and the log2 of mean TPM expression were calculated across all samples. Red dots are DEGs respecting a $\log_2$ fold change >= 1.5 across all 4 DE analysis.

Droplet-based scRNA-seq

Droplet-based single-cell (sc) RNA sequencing were performed at the Centre of Genomic Science, The University of Hong Kong. For scRNA-seq of mouse cells, GemCode Single Cell Platform based on the GemCode Gel Bead was used to process the single cells. Chip and Library Kits (10X Genomics, Pleasanton) was used according to the manufacturer's protocol. In brief, after cell sorting, cells were partitioned into Gel Beads in Emulsion in the GemCode instrument, followed by cell lysis and barcoded reverse transcription of RNA. Finally, amplification, shearing and 5'adaptor and sample index attachment were performed. Libraries were purified and sequenced on an Illumina™ NextSeq 500 according to the standard protocol as suggested by the manufactor.

Computational analysis

Pre-processing of droplet-based scRNA-seq data

Cellranger toolkit (version 3.0) provided by 10X Genomics were used to perform the reads de-multiplexing and alignment. unique molecular identifier (UMI) were counted by aligning to the mouse mm10 transcriptome. For the quality control, only cells with more than 800 detected genes were retained. Genes expressed in more than 10 cells were kept for further analysis. Clustering and marker identification were performed by the Seurat R package(*54*). The integrative analysis of the 3 public dataset was also performed by Seurat.

Single cell trajectory analysis

Single cell trajectory was analyzed by Monocle 3. Before monocle analysis, we removed the ENMFB cells which are separated to neuronal and glial lineages. Low quality cells with few

detected genes and UMIs were also filtered. Top 1500 highly variable genes were used as the features to perform the trajectory analysis. Linear regressions were fitted between gene expression and pseudotime to quantify the changing rate of genes along pseudotime in the scatter plot. Slope and significance were marked in the scatter plot.

PCA and t-SNE analysis
Principal component analysis (PCA) and t-SNE (t-distributed Stochastic Neighbor Embedding) were performed using the Seurat package. We ran PCA using the expression matrix of the top 1,500 most variable genes. t-SNE was then performed on the first 10 principal components with default parameters to visualize cells in a two-dimensional space.

DEG and pathway enrichment analysis
DEG analysis on scRNA-seq dataset was performed by SCDE(*55*). Gene ontology (GO) term enrichment analyses were performed using clusterProfiler R package(*56*). Terms that had a P-value < 0.05 was defined as significantly enriched.

Transcriptomic timing analysis
After the transcriptomic trajectory was learned by Monocle 3 using single-cell expression data. A Bayesian linear regression model was applied to detect "switch-like" upregulation or downregulation of genes along the pseudotime axis. Crucially, the model probabilistically assigns a region along the axis associated with the positive or negative activation of each of each gene in the core gene set.

TF motif enrichment analysis
HOMER (findmotifs.pl function) was used to perform the TF motif enrichment analysis(*57*). To obtain neuronal progenitor-specific target genes, we overlapped the putative target genes identified from HOMER and the public ChIP-seq data from Cistrome(*34*).

Ezh2 activated and repressed target genes prediction
We applied a three-step strategy to obtain the target genes of *Ezh2* during mouse ENCC development at E13.5. For the activated genes, we first got the significantly positively correlated genes with *Ezh2*. Secondly, we only kept the target genes that were supported by the motif enrichment analysis. Lastly, we got the significantly up-regulated DEGs since *Ezh2* is up-regulated in *Kif7 cKO* mutant cells. The same strategy was used to identifying the repressed target genes except for the motif enrichment step.

Statistical Analysis
The differences among multiple treatment groups were analyzed with a two-sided unpaired Student t test or one-way ANOVA followed by Tukey post-test using GraphPad Prism 7 (GraphPad Software). A *p*-value less than 0.05 was interpreted to represent a statistically significant difference. All experiments were replicated at least three times and data are shown as means with standard error of mean (SEM).

Table S4. Primary antibodies used in this study

Primary antibodies	Target antigen	Dilution	Application	Category No.	RRID
Goat-anti-Ret	Receptor tyrosine kinase	1:100	IHC	Neuromics (GT15002)	AB_2179886
Mouse-anti-Tuj1	Neuronal classIII β-tubulin	1:500	IHC	Biolegend (801202)	AB_10063408
Mouse-anti-HuD	ELAV Like RNA Binding Protein 4	1:200	IHC	Santa Cruze (SC-28299)	AB_627765
Rabbit-anti-GFAP	Glial Fibrillary Acidic Protein	1:200	IHC	Dako Cytomation (Z0334)	AB_10013382
Rabbit-anti-Calretinin	Calretinin	1:100	IHC	Swant (CR7697)	AB_2619710
Rabbit-anti-nNOS	nNOS	1:100	IHC	Life Technologies (617000)	AB_2313734
Rabbit-anti-S100β	A member of the S100β family of proteins	1:100	IHC	Dako Cytomation (Z0311)	AB_10013383
Mouse-anti-Ki67	Prototypic cell cycle related nuclear protein	1:100	IHC	BD Pharmingen (556003)	AB_396287
Mouse-anti-HuC/D	RNA-binding protein of the embryonic lethal abnormal visual (Elav) family	1:200	IHC	Invitrogen (21272)	AB_1500232
Rabbit-anti-Bfabp	Fatty acid binding protein 7	1:10000	IHC	A gift from Brunet, J.F, CNRS UMR, Paris, France	N.A.
Mouse-anti-SMA	Smooth muscle	1:200	IHC	Dako Cytomation (M0851)	AB_2223500
Guinea pig-anti-Sox10	SOX (SRY-related HMG-box) family transcription factors Sox10	1:500	IHC	A gift from Prof. Michael Wegner	AB_2721917
Mouse-anti-Sox10	SOX (SRY-related HMG-box) family transcription factors Sox10	1:100	IHC/ICC	Atlas Antibodies (AMAb91297)	AB_2665884
Goat-anti-Phox2b	Paired-like homeobox 2b	1:200	IHC/ICC	R&D Systems (AF4940)	AB_10889846
Rabbit-anti-Ezh2	Enhancer Of Zeste 2 Polycomb Repressive Complex 2 Subunit	1:200	IHC	Cell Signaling Technology (5246S)	AB_10694683
Sheep-anti-GFP	Green fluorescent protein	1:100	IHC	Bio-Rad (4745-1051)	AB_619712
Rabbit-anti-Tuj1	Neuronal classIII β-tubulin	1:200	ICC	Abcam (ab18207)	
Rabbit-anti-GFP	Green Fluorescent Protein	1:100	IHC	Thermofishers (A11122)	AB_444319
Rabbit-anti-Gli1	Gli1 (Hh signaling)	1:500	WB	Santa Cruze (sc-20687)	AB_2111764
Goat-anti-Gli2	Gli2 (Hh signaling)	1:500	WB	R&D (AF3635)	AB_2111902
Rabbit-anti-Gli3	Gli3 (Hh signaling)	1:500	WB	Santa Cruze (sc-20688)	AB_2109708
Mouse-anti-Actin	β-Actin	1:2000	WB	Millipore (MAB1501)	AB_2223041
CD271-APC	Neurotrophin receptor $p75^{NTR}$	1:100	Flow cytometry	Miltenyi Biotec (130110078)	AB_2656849
CD271-FITC	Neurotrophin receptor $p75^{NTR}$	1:100	Flow cytometry	Miltenyi Biotec (130091917)	AB_871651
HNK1-APC	CD57	1:100	Flow cytometry	BD Biosciences (560845)	AB_10563760
Integrin alpha-FITC	Alpha subunit	1:100	Flow cytometry	Abcam (ab25796)	AB_2129610

Table S5. Secondary antibodies used in this study

Secondary antibody	Dilution	Application	Category No.
Alexa Fluor® 488 Donkey-anti-rabbit IgG (H+L)	1:200	IHC	Invitrogen (A21206)
Alexa Fluor® 488 Donkey-anti-mouse IgG (H+L)	1:200	IHC	Invitrogen (A21202)
Alexa Fluor® 594 Donkey-anti-rabbit IgG (H+L)	1:200	IHC	Invitrogen (A21207)
Alexa Fluor® 594 Donkey-anti-mouse IgG (H+L)	1:200	IHC	Invitrogen (A21203)
Alexa Fluor® 647 Donkey-anti-mouse IgG (H+L)	1:200	IHC	Invitrogen (A31571)
Alexa Fluor® 488 Donkey-anti-guinea pig IgG (H+L)	1:200	IHC	Sigma (SAB4600033)
Goat-anti-rabbit HRP	1:2000	WB	Dako Cytomation (P0448)
Goat-anti-mouse HRP	1:2000	WB	Dako Cytomation (P0447)
Rabbit-anti-goat HRP	1:2000	WB	Dako Cytomation (P0449)

Table S6. Sequence Information on Polymerase Chain Reaction Primers

Gene	Primer sequence (5'-3')	Product size (bp)	Annealing temperature (°C)	Cycle	Purpose
Kif7 ex3-4	5'-GTGGATGTAGAAGGCCTGGAC-3' 5'-GCAGGCGATCATCACTGTC-3'	426	64	35	RT-PCR
β-Actin	5'-GAGAGGGAAATCGTGCGTGAC-3' 5'-AGCTCAGTAACAGTCCGCCTA-3'	300	60	35	RT-PCR
Gli1	5'-ACGCCTTGAAAACCTCAAGA-3' 5'-GCAACCTTCTTGCTCACACA-3'	80	60	40	qRT-PCR
Gli2	5'-AGCCCATGACTCTCACCTCCAT-3' 5'-TCGCTGTTCTGCTTGTTCTGGTT-3'	186	60	40	qRT-PCR
Ptch1	5'-GGGTCCTCGCTTACAAACTC-3' 5'-ATGATGCCATCTGCGTCTAC-3'	100	60	40	qRT-PCR
18S	5'-CGGCTACCACATCCAAGGA-3' 5'-GCTGGAATTACCGCGGCT-3'	183	60	40	CyberqRT-PCR